

AD-A038 107

MASSACHUSETTS INST OF TECH CAMBRIDGE FRANCIS BITTER --ETC F/G 20/6  
DEVELOPMENT OF HIGH-POWER TUNABLE SOURCES IN THE 12 MICROMETERS--ETC(U)  
JUL 76 B LAX

N00014-75-C-0558

NL

UNCLASSIFIED

1 OF 1  
ADAO38107



END

DATE  
FILMED  
4-77

ADA038107

395-592  
4 ap  
2-19-76

Massachusetts Institute of Technology  
FRANCIS BITTER NATIONAL MAGNET LABORATORY

FINAL TECHNICAL REPORT

DEVELOPMENT OF HIGH-POWER TUNABLE SOURCES  
IN THE 12  $\mu$ m AND 16  $\mu$ m REGIONS

Micrometers

Sponsored by

Advanced Research Projects Agency

ARPA Order No. 2840

Program Code No. 5E20

Contract No. N00014-75-C-0558

Scientific Officer  
Director, Physics Program  
Physical Sciences Division  
Office of Naval Research  
800 North Quincy Street  
Arlington, VA 22217

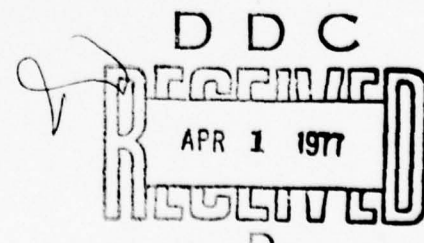
Principal Investigator

10 Benjamin Lax  
Benjamin Lax, Director  
Francis Bitter National Magnet Laboratory  
Professor of Physics  
Tel. (617) 253-5541

APPROVED FOR PUBLIC RELEASE; DISTRIBUTION UNLIMITED.

12 27p.

11 July, 1976



AD NO. 1  
DDC FILE COPY

WORKSHEET

White Section

Buff Section

Per FL-88 (R77-0270) on file

dtg. 10 Feb. 77

This report is a summary of the work done under the project

"Development of High-Power Tunable Sources in the 12  $\mu\text{m}$  and 16  $\mu\text{m}$  Regions".

As shown in Appendix A, we have successfully demonstrated the generation of 12  $\mu\text{m}$  radiation by two-step difference-frequency mixing of  $\text{CO}_2$  laser radiation in GaAs. With 3 MW peak input power from each of the two  $\text{CO}_2$  lasers operating at 9.6  $\mu\text{m}$  and 10.6  $\mu\text{m}$ , peak output power of  $\sim 4$  kW was obtained at 11.8  $\mu\text{m}$ . In this scheme, at first two  $\text{CO}_2$  laser beams of frequencies  $\omega_1$  and  $\omega_2$  with  $\omega_1 > \omega_2$  are used to generate far-infrared (FIR) radiation at the difference-frequency  $\omega_3 = \omega_1 - \omega_2$  in the 100  $\mu\text{m}$  region by noncollinear phase-matched mixing in a GaAs crystal of "folded parametric" geometry. This FIR radiation is then mixed simultaneously with another  $\text{CO}_2$  laser beam of frequency  $\omega_2$  in the same crystal of GaAs. This results in the difference-frequency infrared radiation at  $\omega_4 = 2\omega_2 - \omega_1$  in the 12  $\mu\text{m}$  region. Thus the efficiency of 12  $\mu\text{m}$  radiation generation by two step difference-frequency mixing depends upon the efficiency for the generation of the FIR radiation. As shown in Appendix B, as much as 4 kW FIR output at 100  $\mu\text{m}$  was generated with about 1.7 MW and 3 MW peak power from the two  $\text{CO}_2$  input lasers. This output power level is several orders of magnitude higher than those reported previously.<sup>1-3</sup> But the FIR output is still more than an order of magnitude less than the theoretical estimate which does not include the absorption losses for the input and output beams. Recently<sup>4</sup> we have measured the absorption coefficient

DISTRIBUTION STATEMENT A

Approved for public release;  
Distribution Unlimited

of GaAs at liquid helium temperature with a Fourier transform interferometer. The results show that the absorption coefficient of GaAs at 13°K is less than  $0.08 \text{ cm}^{-1}$  at  $100 \mu\text{m}$ . This absorption coefficient is too small to account for the discrepancy between calculated and observed values for the FIR power output.

We have developed an efficient new scheme for the generation of infrared radiation with potential application to the uranium isotope separation program. As shown in Appendix C, we have demonstrated the noncollinear phase-matched 4-photon mixing in germanium. Approximately 1 mJ of energy per pulse was obtained at  $8.7 \mu\text{m}$  from an 8.3 cm long crystal of germanium at room temperature with  $1 \text{ cm}^2$  cross-section and  $3 \text{ MW/cm}^2$  peak input intensity from each of two  $\text{CO}_2$  TEA lasers. In Appendix D, we examine the possibility of this room temperature mixing scheme as a potential infrared source for the uranium isotope separation in  $\text{UF}_6$ . The possibility appears to be very promising. We have carried out a similar 4-photon experiment for the generation of  $12 \mu\text{m}$  radiation. Unfortunately the observed value is much below the theoretical estimate. Again the absorption coefficient of Ge at  $12 \mu\text{m}$  region cannot account for the discrepancy between theory and experiment.

A considerable effort was devoted towards the development of the desired  $\text{CO}_2$  laser system for optical mixing experiments. We fabricated a pair of synchronized single longitudinal mode megawatt  $\text{CO}_2$  hybrid lasers. Also by using a tilted intracavity GaAs etalon, we have achieved single longitudinal mode operation of a  $\text{CO}_2$  laser

with fine tuning capability over the pressure broadened gain curve ( $\sim 4.5$  MHz/torr or  $\sim 3.5$  GHz at atmospheric pressure). This fine tuning could provide the optimal frequency of the  $8.62\text{ }\mu\text{m}$  for the uranium isotope separation of  $\text{UF}_6$ .

In summary, the work done under project has contributed to the following two patent applications and a number of journal publications.

A. Patent Applications

1. Method of and Apparatus for Generating Tunable Coherent Radiation by Nonlinear Light Mixing in Systems Having Folded Noncollinear Geometries.
2. Method of and Apparatus for Generating Tunable Radiation by Noncollinear Phase-Matched Sum-Difference Frequency Optical Mixing.

B. Journal Articles

1. Generation of  $12\text{ }\mu\text{m}$  Radiation by Difference-Frequency Mixing of  $\text{CO}_2$  Laser Radiation in GaAs; Appl. Phys. Lett. 29, 45 (1976).

2. High Power Far Infrared Generation in GaAs, Opt. Commun. 18, 50 (1976).
3. Noncollinear Phase-Matched Four Photon Generation of CO<sub>2</sub> Laser Radiation in Germanium, submitted to Appl. Phys. Lett.
4. <sup>micrometers</sup> and Efficient High-Power 8.62  $\mu\text{m}$  Infrared Radiation Source for Uranium Isotope Separation in UF<sub>6</sub>, to appear in Proceedings of the International Conference on Lasers and their Applications, Leon, Norway, 1976.
5. Fine Tuning of a Single Longitudinal Mode CO<sub>2</sub> TEA Laser, to be submitted.

References:

1. R.L. Aggarwal, B. Lax and G. Favrot, Appl. Phys. Lett. 22, 329 (1973).
2. B. Lax, R.L. Aggarwal and G. Favrot, Appl. Phys. Lett. 23, 679 (1973).
3. N. Lee, R.L. Aggarwal and B. Lax, Opt. Commun. 11, 339 (1974).
4. R.W. Flanagan, M.S. Thesis, Massachusetts Institute of Technology, 1976 (unpublished).

## APPENDIX A

Generation of  $12 \mu\text{m}$  Radiation by Difference-Frequency

Mixing of  $\text{CO}_2$  Laser Radiation in GaAs

# Generation of 12- $\mu\text{m}$ radiation by difference-frequency mixing of $\text{CO}_2$ laser radiation in GaAs<sup>†</sup>

JP 693

N. Lee, R. L. Aggarwal,\* and B. Lax\*

Francis Bitter National Magnet Laboratory,<sup>†</sup> Massachusetts Institute of Technology, Cambridge  
Massachusetts 02139

(Received 25 March 1976)

Step-tunable infrared radiation in the 12- $\mu\text{m}$  region can be generated by two-step noncollinear difference-frequency mixing of  $\text{CO}_2$  laser beams in GaAs at liquid-helium temperature. With 3-MW peak input power from each of the two  $\text{CO}_2$  lasers operating at 9.6 and 10.6  $\mu\text{m}$ , peak output power of  $\sim 4$  kW was obtained at 11.8  $\mu\text{m}$ .

PACS numbers: 42.65.-k, 42.50.+q, 42.60.Nj

In this letter we report the use of a two-step noncollinear difference-frequency mixing of  $\text{CO}_2$  laser beams in GaAs for the generation of infrared radiation in the 12- $\mu\text{m}$  region. At first two  $\text{CO}_2$  laser beams of frequencies  $\omega_1$  and  $\omega_2$  with  $\omega_1 > \omega_2$  are used to generate far-infrared (FIR) radiation at the difference-frequency  $\omega_3 = \omega_1 - \omega_2$  by noncollinear phase-matched mixing in a GaAs crystal of "folded parametric" geometry.<sup>1-3</sup> This FIR radiation is then mixed simultaneously with another  $\text{CO}_2$  laser beam of frequency  $\omega_2$  in the same crystal of GaAs. This results in the difference-frequency infrared radiation at  $\omega_4 = \omega_2 - \omega_3 = 2\omega_2 - \omega_1$ . The wave-vector diagram for this two-step difference-frequency mixing inside the GaAs crystal is shown in Fig. 1.  $\mathbf{k}_1$  is the wave vector for the input beam at  $\omega_1$ ,  $\mathbf{k}_2$  and  $\mathbf{k}_2''$  are the wave vectors for the two input beams at  $\omega_2$ ,  $\mathbf{k}_3$  and  $\mathbf{k}_4$  are the wave vectors for the radiation generated at  $\omega_3$  and  $\omega_4$ , respectively. With  $\omega_1$  and  $\omega_2$  in the 9.6- $\mu\text{m}$  and 10.6- $\mu\text{m}$  regions, respectively, this two-step difference-frequency mixing provides radiation in the 12- $\mu\text{m}$  region with  $\omega_3$  in the 100- $\mu\text{m}$  region.

The GaAs crystal used in this work was prepared by optical contacting three separately polished pieces of high-resistivity Cr-doped GaAs<sup>4</sup> as shown in Fig. 2. The transmission loss for each optically contacted interface was determined to be less than a few percent for the  $\text{CO}_2$  laser radiation. The nonlinear mixing takes place in the long piece A which was 100 mm in length and 5 mm in width. Pieces B and C which serve to couple the radiation in and out of piece A were 25 mm in length and 14 mm in width. The input and output faces b and c were cut at an angle of 22° as shown in Fig. 2. Surfaces

$a_1$ ,  $a_2$ ,  $a_3$ , and  $a_4$  of the piece A along with input and output surfaces b and c had been polished to  $\lambda/20$  flatness for the  $\text{CO}_2$  laser radiation. The surfaces  $a_3$  and  $a_4$ , which are responsible for the total internal reflection of the  $\text{CO}_2$  laser beams, were made plane parallel to within 20 arc sec. The section of the crystal shown in Fig. 2 is in a (111) crystallographic plane. All the three pieces of GaAs were 10 mm in height along a [111] direction which is arranged to be parallel to the polarization vector of the three incident laser beams. The crystal was cooled to liquid-helium temperatures by mounting it on a 4-in. cold finger of a liquid-helium dewar.

The schematic of the experimental setup is shown in Fig. 3. The  $\omega_1$  and  $\omega_2$  beams were provided by a pair of synchronized  $\text{CO}_2$  TEA lasers equipped with diffraction gratings. These lasers have a maximum output of  $\sim 1$  J at repetition rates up to 1 pps. The temporal jitter between the two  $\text{CO}_2$  laser pulses was less than 30 nsec for most of the pulses. The  $\omega_2$  beam was divided into two beams  $\omega_2'$  and  $\omega_2''$  by means of a germanium beam splitter. The  $\omega_2'$  beam is incident on the input face b in Fig. 3 at the external phase-matching angle  $\theta_{1F}$  relative to the  $\omega_1$  beam.<sup>1</sup> The FIR radiation was monitored by a Laser-Precision pyroelectric radiometric detector model kT-4020S or pyroelectric joule meter model Rkp-335. The FIR output was maximized by an adjustment of  $\theta_{1F}$  with a cam-controlled mirror  $M_1$  and fine rotation of the crystal about a vertical axis lying in the input face b.

The  $\omega_2''$  beam was incident at an external angle  $\delta_F$  with respect to the  $\omega_1$  beam as shown in Fig. 3. The adjustment of  $\delta_F$  was accomplished by a mirror  $M_2$  which is similar to  $M_1$ . The output of the infrared radiation at  $\omega_4$  was measured by the same pyroelectric detectors used for the monitoring of the FIR radiation. Long wave pass interference filters were used to reject the input

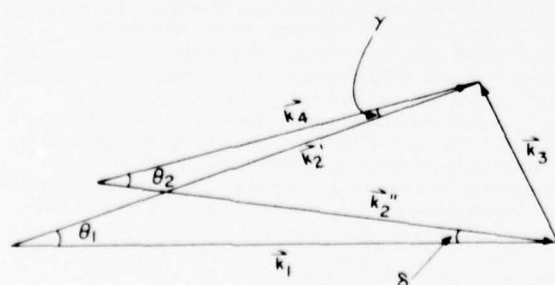


FIG. 1. Wave-vector diagram showing the directions of propagation of the incident beams  $\mathbf{k}_1$ ,  $\mathbf{k}_2$ , and  $\mathbf{k}_2''$  and the generated difference-frequency beams  $\mathbf{k}_3$  and  $\mathbf{k}_4$  inside the GaAs crystal.

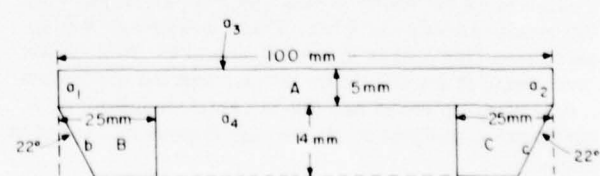
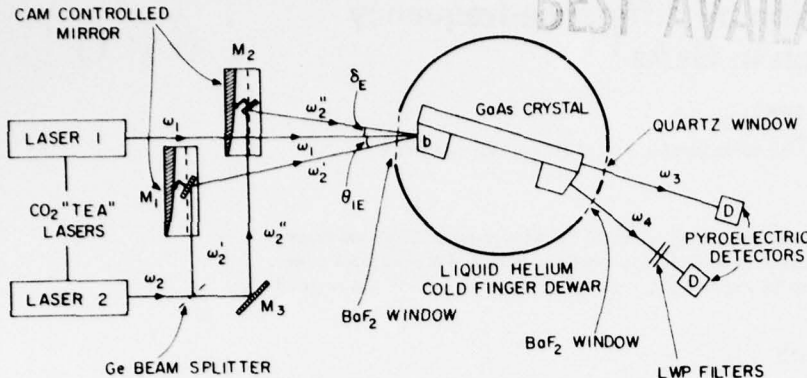


FIG. 2. Geometry of the GaAs crystal prepared in the folded parametric configuration.



CO<sub>2</sub> laser radiation and its harmonics in the 5-μm region.

Neglecting absorption and all other losses for the input and output beams, the external output power at  $\omega_4$  is given in mks units by

$$P_{\omega_4} = \left( \frac{\mu_0}{\epsilon_0} \right) \frac{\omega_2^2 \omega_1^2 L^4 A_4}{16 n_1 n_2 n_3 n_4 c^4} \times \left( 2d_{\text{eff}} \right)^4 g_3^2 g_4^2 \left( \frac{P_{\omega_1}}{A_1} \right) \left( \frac{P_{\omega_2}}{A_2} \right) \left( \frac{P_{\omega_2''}}{A_2''} \right) T_1 (T_2)^2 T_4, \quad (1)$$

where  $\mu_0$  and  $\epsilon_0$  are the magnetic and electric permeabilities of vacuum.  $n_1$ ,  $n_2$ ,  $n_3$ , and  $n_4$  are indices of refraction of GaAs at frequencies  $\omega_1$ ,  $\omega_2$ ,  $\omega_3$ , and  $\omega_4$ , respectively.  $c$  is the velocity of light.  $d_{\text{eff}}$  is the effective second-order nonlinear coefficient.  $g_3$  and  $g_4$  are the geometrical factors for the generation of  $\omega_3$  and  $\omega_4$ , respectively, and have the values of 2 and 1.1 in our particular case.<sup>2</sup>  $P_{\omega_1}$ ,  $P_{\omega_2}$ , and  $P_{\omega_2''}$  are the external peak powers in the  $\omega_1$ ,  $\omega_2$ , and  $\omega_2''$  beams as incident on GaAs, and  $A_1$ ,  $A_2$ , and  $A_2''$  are the corresponding input beam cross sections.  $A_4$  is the cross section of the output beam at  $\omega_4$ .  $T_1$ ,  $T_2$ , and  $T_4$  are the single surface transmission coefficients at the frequencies  $\omega_1$ ,  $\omega_2$ , and  $\omega_4$ .  $L$  is the length of the crystal over which the nonlinear mixing occurs.

Using CO<sub>2</sub> laser lines P22 and P18 in the 9.6 μm and 10.6 μm, respectively, corresponding to  $\omega_1 = 1045.02$  cm<sup>-1</sup>,  $\omega_2 = 945.98$  cm<sup>-1</sup>,  $\omega_3 = 99.04$  cm<sup>-1</sup>, and  $\omega_4 = 846.94$  cm<sup>-1</sup>, both  $P_{\omega_3}$  and  $P_{\omega_4}$  were determined<sup>5</sup> to be ~4 kW for input powers  $P_{\omega_1} \approx 3$  MW,  $P_{\omega_2} = P_{\omega_2''} = 1.7$  MW with beam cross sections  $A_1 \approx A_2 \approx A_2'' \approx A_4 = 1$  cm<sup>2</sup>. Using  $d_{\text{eff}} = (2/\sqrt{3})d_{14}$  for the [111] polarization of the input and output beams with a value<sup>6</sup> of  $43 \times 10^{-12}$  m/V, and  $n_1 \approx n_2 = 3.31$ ,  $n_3 \approx 3.66$ ,  $n_4 \approx 3.30$ ,  $L = 7.5$  cm along with other values for the above parameters, Eq. (1) predicts a value of 18 kW which is about 4–5 times larger than the measured value of 4 kW. This discrepancy may in part arise from phase mismatch due to the finite beam divergence of the CO<sub>2</sub> laser beams, and the absorption losses at all infrared and far-infrared frequencies. A quantitative analysis of all the loss factors has yet to be made.

FIG. 3. Schematic of the experimental setup for the two-step difference-frequency mixing in GaAs at liquid-helium temperature. For  $\omega_1 = 1045$  cm<sup>-1</sup> and  $\omega_2 = 946$  cm<sup>-1</sup>,  $\theta_{IE} \approx 8^\circ$ ,  $\delta_E \approx 1.6^\circ$ .

A CO<sub>2</sub> laser can be tuned to a whole series of discrete lines from ~9 to 11 μm in the *P* and *R* branches of the 10.4- and 9.4-μm bands. We have demonstrated the tunability of the FIR radiation by difference-frequency mixing of two CO<sub>2</sub> lasers with frequency spacing as small as 0.01 cm<sup>-1</sup> when both the CO<sub>2</sub> lasers are simultaneously step tuned by a line at a time. Similar tunability can be obtained for the generation of infrared radiation at  $\omega_4 = 2\omega_2 - \omega_1$  by selecting different combinations of CO<sub>2</sub> laser lines for the input  $\omega_1$  and  $\omega_2$  beams. However, there is a practical limitation on the fine tunability as well as the range of tunability for the  $\omega_4$  generation, since the intensity of  $\omega_4$  depends upon the intensity of the FIR radiation generated at the frequency  $\omega_3$  which is in turn proportional to  $\omega_3^2$ . For a given  $\omega_4$ , therefore, it is desirable to choose the input frequencies  $\omega_1$  and  $\omega_2$  which provide the largest value of  $\omega_3$ . On the other hand, the FIR absorption loss in GaAs increases with increasing  $\omega_3$ , particularly for frequencies above 100 cm<sup>-1</sup>. In view of these opposing factors, the optimal region for the generation of  $\omega_3$  is around 100 cm<sup>-1</sup>. Taking  $\omega_3$  in the 60–110-cm<sup>-1</sup> region,  $\omega_4$  would span the frequency range from 970 to 810 cm<sup>-1</sup>, corresponding to wavelengths between 10.3 and 12.3 μm.

Work supported in part by the Advanced Research Projects Agency through the Office of Naval Research and in part by the National Science Foundation.

\*Also Physics Department, M.I.T.

†Supported by the National Science Foundation.

<sup>1</sup>R. L. Aggarwal, B. Lax, and G. Favrot, *Appl. Phys. Lett.* **22**, 329 (1973); **23**, 679 (1973).

<sup>2</sup>N. Lee, R. L. Aggarwal, and B. Lax, *Opt. Commun.* **11**, 339 (1974).

<sup>3</sup>N. Lee, B. Lax, and R. L. Aggarwal, Conference Summary of the IX International Conference on Quantum Electronics, Amsterdam, 1976 [Opt. Commun. (to be published)].

<sup>4</sup>GaAs crystals were supplied by Crystal Specialties, Monrovia, Calif. Polishing and optical contacting work was done by Laser Optics, Danbury, Conn.

<sup>5</sup>The input peak powers given here have been deduced on the assumption that half of the CO<sub>2</sub> pulse energy is contained in an initial spike of 100 nsec (FWHM) with the remaining half of the energy in a relatively long tail. The output peak powers were obtained by assuming that the output energy was contained in a 100-nsec (FWHM) pulse.

<sup>6</sup>G. D. Boyd, T. J. Bridges, M. A. Pollack, and E. H. Turner, *Phys. Rev. Lett.* **26**, 387 (1971).

APPENDIX B

High Power Far Infrared Generation in GaAs

Optics Communications 18, 50 (1976)

The focal spot size is chosen to give a combined incident power density of approximately  $5 \text{ MW cm}^{-2}$ , which was found to be below the damage threshold of the crystal for these short pulses. The infrared difference signal is detected with a HgCdTe detector.

To satisfy non-critical ( $90^\circ$ ) phasematching, both dye lasers must be tuned simultaneously. The input wavelengths necessary for each infrared difference frequency were calculated using the Sellmeier equations given by Bahr and Smith [1]. To cover the entire range, the  $\text{o-ray}$  was tuned from  $5385 \text{ \AA}$  to  $5800 \text{ \AA}$  and the  $\text{o-ray}$  from  $5550 \text{ \AA}$  to  $6200 \text{ \AA}$ . The experimentally measured wavelengths were within  $10 \text{ \AA}$  of the calculated ones. This demonstrates that the Sellmeier equation for the infrared, which was derived from index data to 13 microns, is useful to at least 18 microns. The conversion efficiency was found to decrease at about 13 microns, but to rise again at 15 microns. This decrease in efficiency can be attributed to a two phonon absorption [4]. However, this absorption does not limit the usefulness of the crystal in this region, and, in addition, it was found to have only a minimal effect on the indices. The cut-off at 18 microns is due to the detector response.

With one of the dye laser frequencies fixed, the other dye laser was scanned through the corresponding phasematching frequency. The expected  $(\sin x/x)^2$  signature was observed and was measured to have a width (fwhm) of  $5 \text{ cm}^{-1}$ , which agrees with the calculated value to within the bandwidths of the dye lasers.

This experiment demonstrates the feasibility of using a nitrogen laser-dual dye laser combination for tunable infrared generation in the fingerprint region of the infrared. Its relative simplicity and low cost make it an attractive alternative to parametric oscillators and spin-flip Raman lasers.

We wish to thank Prof. R.L. Byer of Stanford Univ. for providing the crystal of  $\text{AgGaS}_2$ .

#### References

- [1] G.C. Bahr and R.C. Smith, *IEEE J. Quantum Electron.* QE-10 (1974) 546.
- [2] S.A. Myers, *Opt. Commun.* 4 (1971) 187.
- [3] D.C. Hanna, P.A. Karkkainen, and R. Wyatt, *Optics and Quant. Elect.* 7 (1975) 115.
- [4] J. Jerphagnon, private communication.

#### F3 HIGH POWER FAR INFRARED GENERATION IN $\text{GaAs}^*$

N. LEE, B. LAX\*\* and R.L. AGGARWAL\*\*

*Francis Bitter National Magnet Laboratory†,  
Massachusetts Institute of Technology, Cambridge,  
Massachusetts 02139, USA*

Previously [1,2] reported generation of far infrared (FIR) radiation by noncollinear mixing of two pulsed TEA  $\text{CO}_2$  lasers in a 1 cm crystal of  $\text{GaAs}$  at liquid helium temperatures produced step-tunable radiation from  $\sim 70 \mu\text{m}$  to 2 mm. With

200 kW input peak power from each  $\text{CO}_2$  laser  $\sim 20 \text{ mW}$  peak output power at a wavelength of  $\sim 100 \mu\text{m}$  was obtained. In this paper we report the generation of FIR output  $\sim 4 \text{ kW}$  at  $\sim 100 \mu\text{m}$ , which is orders of magnitude higher than those obtained previously. These new experimental results were achieved by using noncollinear folded mixing geometries [3].

With a 10 cm long crystal of a simple folded geometry [4] in liquid helium temperatures and 130 kW peak input power incident on the crystal from each  $\text{CO}_2$  laser, the FIR output was measured to be  $\sim 50 \text{ W}$  at  $100 \mu\text{m}$  at the output face of the crystal [5]. This result is within an order of magnitude of the theoretical estimate neglecting the absorption losses. The orders-of-magnitude improvement of present results is largely due to a better  $\text{GaAs}$  crystal and more reliable calibration of the FIR detection system. Much higher input powers could not be used in this crystal since laser damage was observed at an energy density as low as  $0.3 \text{ J/cm}^2$  which is more than an order of magnitude less than the generally quoted value of  $10 \text{ J/cm}^2$ . The cause for this lowering of the damage threshold was found to be due to the trapping of the  $\text{CO}_2$  laser beams inside this crystal geometry. The trapped multiple passed  $\text{CO}_2$  laser beams interfere with each other constructively at some points in the crystal creating high peak intensity regions at the surface.

By going to a folded parametric geometry [6] with input and output couplers for the  $\text{CO}_2$  laser beams, we have eliminated the internal trapping of  $\text{CO}_2$  laser radiation responsible for lower damage threshold. A 10 cm long crystal of folded parametric geometry was prepared by optically contacting input and output couplers for the  $\text{CO}_2$  laser beams to the main crystal. The transmission loss of  $\text{CO}_2$  laser beams across such an optically contacted interface was found to be about one percent. With about 1.7 MW and 3 MW peak power from the two  $\text{CO}_2$  laser beams incident on the sample, we obtained  $\sim 4 \text{ kW}$  FIR power at  $\sim 100 \mu\text{m}$  at the output face of the crystal.

Presently we are developing the fine tuning capability of our TEA lasers so as to take advantage of resonance cavity for FIR radiation. We hope this will improve the mixing efficiency for the FIR generation.

#### References

- [1] R.L. Aggarwal, B. Lax and G. Favrot, *Appl. Phys. Lett.* 22 (1973) 329.
- [2] B. Lax, R.L. Aggarwal and G. Favrot, *Appl. Phys. Lett.* 23 (1973) 679.
- [3] N. Lee, R.L. Aggarwal and B. Lax, *Opt. Commun.* 11 (1974) 339.
- [4] See fig. 2 of ref. [3].

\* Supported in part by the Advanced Research Projects Agency through the Office of Naval Research, and in part by the National Science Foundation.

\*\* Also Physics Department, M.I.T.

† Supported by the National Science Foundation.

[5] The input peak powers given here have been deduced on the assumption that half of the  $\text{CO}_2$  pulse energy is contained in an initial spike of 100 nsec (fwhm) with the remaining half of the energy in a relatively long tail. The FIR peak powers are obtained by assuming that the output energy is contained in a 100 nsec (fwhm) pulse.  
 [6] See figs. 3 of ref. [3].

#### F4 SECOND HARMONIC GENERATION IN RARE-EARTH ION DOPED NONLINEAR CRYSTAL

R. BONNEVILLE and F. AUZEL

Centre National d'Etudes des Télécommunications,  
 196 rue de Paris, 92220 Bagneux, France

Interactions between rare earth ions in solids are known to induce, besides energy transfers, cooperative effects [1]. Among them, cooperative luminescence has been reported by Nakasawa and Shionoya [2]: when exciting  $\text{YbPO}_4$  by incoherent, near infrared ( $\text{Yb}^{3+}$  absorption) light, they observed an anti-stokes luminescence at twice the excitation energy, the intensity of which exhibits a quadratic dependence on the incident flux. The recorded spectra can be understood by considering the coalescence of two excited  $\text{Yb}^{3+}$  ions into one photon of twice their energy.

If this effect could be produced coherently it will be some sort of second harmonic generation and could therefore possibly enhance the nonlinear optical properties of a crystal. Since  $\text{Yb}^{3+}$  absorption is not too far from neodymium-YAG laser at  $1.06 \mu$  [1], our choice as nonlinear host has been gadolinium molybdate (GMO) which already contains rare-earth ions, so that partial substitution of  $\text{Gd}^{3+}$  by  $\text{Yb}^{3+}$  ions is rather easy [3]; good optical quality single crystals can be obtained, though care must be taken to eliminate ferroelastic domains [4].

Nonlinear optical properties of pure GMO have already been investigated [7]. X-ray studies show that GMO in the paraelastic phase has point-group symmetry  $\text{mm}2(\text{C}_{2h})$  and that  $\text{Gd}^{3+}$  site has no symmetry elements (and particularly no inversion center) [8].

The five nonlinear optical coefficients of  $\text{Gd}_{2-x}\text{Yb}_x(\text{MoO}_4)_3$  were measured by a standard Maker's fringes method. A significative enhancement of SHG was observed, variable with the investigated coefficient, from about 30% for  $d_{31}$  and  $d_{32}$ , 60% for  $d_{15}$  and  $d_{24}$ , to more than 100% for  $d_{33}$ , with a 10%  $\text{Yb}^{3+}$  concentration. In order to evaluate theoretically the contribution of  $\text{Yb}^{3+}$  ions to nonlinear susceptibility, and to determine what kind of resonant effect, if any, is involved, several steps in our calculations have been considered:

- Contribution of a one ion resonance in the vicinity of  $1.06 \mu$  alone,
- Contribution of a resonant coherent cooperative emission,
- Contribution due to second harmonic fluorescence from the equivalent rare-earth ions at sites lacking inversion center, enhanced by one ion resonance.

#### References

- [1] F. Auzel, Proc. IEEE 61 (1973) 758.
- [2] E. Nakasawa, S. Shionoya, Phys. Rev. Lett. 25 (1970) 1710.
- [3] H.J. Borchardt, P.E. Bierstedt, Appl. Phys. Letter 8 (1966) 50.
- [4] A. Kumada, Ferroelectrics 3 (1972) 115.  
 R.C. Miller, W.A. Nordland, K. Nassau, Ferroelectrics 2 (1971) 97.
- [5] W. Jeitschko, Acta Cryst. B 28 (1972) 60.

#### F5 MOLECULAR MECHANICS OF THE FERRO-ELECTRIC TO PARAELECTRIC PHASE TRANSITION IN $\text{Ba}_6\text{Ti}_2\text{Nb}_8\text{O}_{30}$ VIA OPTICAL SECOND HARMONIC GENERATION

J.G. BERGMAN  
*Bell Laboratories, Holmdel, New Jersey 07733, USA*

Second harmonic generation (SHG) can be used to determine the positions of atoms in crystals [1]. The essence of the method relies on the simple relation  $I \propto f(\theta)$ , where  $I$  represents the intensity of the 2nd harmonic (the square root of  $I$  is proportional to the bulk nonlinear polarizability  $d$ ) and  $\theta$  represents the relative position of some bond in the unit cell. The aforementioned technique has now been successfully applied to structural problems involving rigid body rotations and deformations of tetrahedra as well as trigonal and tetragonal deformations of octahedra. In the case of the ferroelectric [2] tungsten bronze-type crystal,  $\text{Ba}_6\text{Ti}_2\text{Nb}_8\text{O}_{30}$  we find that the

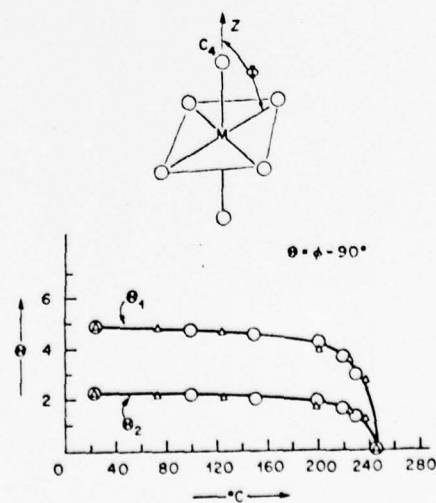


Fig. 1. Temperature dependence of the  $\text{MO}_6$  distortion angle  $\theta$  ( $\theta = \phi - 90^\circ$ ) as determined from the SHG coefficient  $d_{333}$  ( $\text{O}'s$ ) and the spontaneous polarization  $P_z$  ( $\Delta's$ ).

APPENDIX C  
Noncollinear Phase-Matched Four Photon Mixing  
of CO<sub>2</sub> Laser Radiation in Germanium

(Submitted to Applied Physics Letters )

Noncollinear Phase-Matched Four Photon Mixing  
of CO<sub>2</sub> Laser Radiation in Germanium\*

N. Lee, R.L. Aggarwalt, and B. Lax†

Francis Bitter National Magnet Laboratory‡  
Massachusetts Institute of Technology  
Cambridge, Massachusetts 02139

Abstract

Noncollinear four photon mixing of two TEA CO<sub>2</sub> laser beams in germanium at room temperature has been used to obtain phase-matched generation of step tunable radiation in the 8.7  $\mu\text{m}$  region which is of interest for the uranium isotope separation. Using an 8.3 cm long crystal of germanium, peak output power of  $\sim 10$  kW (corresponding to 1 mJ per pulse) was obtained at 8.7  $\mu\text{m}$  with 3 MW peak input power from each of the two CO<sub>2</sub> lasers operating at 9.6  $\mu\text{m}$  and 10.6  $\mu\text{m}$ .

\*Work supported in part by Massachusetts Institute of Technology funds and in part by the Advanced Research Projects Agency through the Office of Naval Research.

†Also Physics Department, M.I.T.

‡Supported by the National Science Foundation.

Germanium is perhaps one of the best materials for the generation of radiation in the 8 to 13  $\mu\text{m}$  region via the four photon mixing of  $\text{CO}_2$  laser beams. This is due to its relatively large third-order nonlinear susceptibility<sup>1-4</sup>, availability of high-purity single crystals in large sizes<sup>5</sup> and high transparency in the above spectral region.<sup>6</sup> It should be pointed out that the 8 to 13  $\mu\text{m}$  wavelength region includes the 8.62  $\mu\text{m}$  and 12.1  $\mu\text{m}$  wavelengths which are important for isotope separation in  $\text{UF}_6$ <sup>7</sup>. In this letter we report the use of noncollinear 4-photon mixing of two TEA  $\text{CO}_2$  laser beams in a long crystal of germanium at room temperature to obtain phase-matched generation of step-tunable high-power radiation in the 8.7  $\mu\text{m}$  region.

Consider two  $\text{CO}_2$  lasers operating at the frequencies  $\omega_1$  and  $\omega_2$  with  $\omega_1 > \omega_2$ . Then the phase-matching condition for the 4-photon mixing  $\omega_3 = 2\omega_1 - \omega_2$  requires

$$\vec{k}_3 = 2\vec{k}_1 - \vec{k}_2, \quad (1)$$

where  $\vec{k}_1$  and  $\vec{k}_2$  are the wave vectors for the input laser beams of frequencies  $\omega_1$  and  $\omega_2$  respectively.  $\vec{k}_3$  is the wave vector for the radiation generated at the frequency  $\omega_3$ . Since  $|\vec{k}| = \frac{n\omega}{c}$ , the phase-matching angle  $\theta$  (inside the crystal) between the  $\omega_1$ - and  $\omega_2$ -beams, as shown in Fig. 1, is given by

$$\cos \theta = \frac{(2n_1\omega_1)^2 + (n_2\omega_2)^2 - (n_3\omega_3)^2}{4n_1n_2\omega_1\omega_2} \quad (2)$$

where  $n_1$ ,  $n_2$ , and  $n_3$  are the refractive indices at  $\omega_1$ ,  $\omega_2$ , and  $\omega_3$  respectively. Similarly, the angle  $\varphi$  of the generated  $\omega_3$ -beam with respect to the  $\omega_1$ -beam is given by

$$\cos \varphi = \frac{(2n_1\omega_1)^2 + (n_3\omega_3)^2 - (n_2\omega_2)^2}{4n_1n_3\omega_1\omega_3} \quad (3)$$

For  $n_1 \approx n_2 \approx n_3$ , Eqs. (2) and (3) can be expressed as

$$\theta \approx \left[ \frac{2(n_3 - n_1)}{n_1} \cdot \frac{2\omega_1}{\omega_2} + \frac{2(n_3 - n_2)}{n_1} \cdot \frac{\omega_2}{2\omega_1} \right]^{1/2} \quad (4a)$$

and

$$\varphi \approx \frac{\omega_2}{\omega_3} \theta \quad (4b)$$

Using the refractive index data for germanium<sup>8</sup>, the angles  $\theta$  and  $\varphi$  can be shown to be less than 1° for the 4-photon mixing of CO<sub>2</sub> laser beams in germanium.

The schematic of the experimental setup is shown in Fig. 2.

The  $\omega_1$ - and  $\omega_2$ -beams were provided by a pair of synchronized TEA CO<sub>2</sub> lasers as described previously.<sup>9</sup> Germanium crystal used in this work was Sb-doped with resistivity in the 5 to 30 ohm-cm range and room temperature absorption coefficient  $\alpha \leq 0.03 \text{ cm}^{-1}$  at 10.6  $\mu\text{m}$ .

The crystal was 8.3 cm long with 1.5 cm square in cross-section.

Both the input and output faces were lapped and polished parallel to each other. The section of the crystal shown in Fig. 2 is in a (111) crystallographic plane which is arranged to be perpendicular to the polarization vectors of the two CO<sub>2</sub> laser beams.

The  $\omega_1$ -beam was directed normal to the input face of the germanium crystal. The  $\omega_2$ -beam was incident on the input face of the Ge crystal at the external phase-matching angle  $\theta_E \approx n_2 \theta$  relative to the  $\omega_1$ -beam. The peak output power at  $\omega_3$  was monitored by a Laser Precision pyroelectric radiometric detector model kT-4020S. Short wave pass interference filters were used to reject scattered radiation at the input frequencies  $\omega_1$  and  $\omega_2$ . The  $\omega_3$  output was maximized by an adjustment of  $\theta_E$  with a cam controlled mirror  $M_2$ . The total energy in a given  $\omega_3$  pulse was also measured with a Gentec joulemeter model ED-200.

Under phase-matched conditions, the peak output power at  $\omega_3$  is given in CGS units by<sup>1,2</sup>

$$P_{\omega_3} = \frac{256 \pi^4 (\omega_3)^2 A_3}{n_1^2 n_2 n_3 c^4} \left( 3 \chi_{1111}^{(3)} \right)^2 \left( \frac{P_{\omega_1}}{A_1} \right)^2 \left( \frac{P_{\omega_2}}{A_2} \right)^2 T_1^2 T_2 T_3 e^{-\alpha_3 L} \left( \frac{1 - e^{-\Delta\alpha L}}{\Delta\alpha L} \right)^2 L^2 \quad (5)$$

with  $\Delta\alpha = \frac{1}{2}(2\alpha_1 + \alpha_2 - \alpha_3)$

where  $\chi_{1111}^{(3)}$  is the effective third-order nonlinear coefficient.  $P_{\omega_1}$  and  $P_{\omega_2}$  are the external peak input powers of the  $\omega_1$  and  $\omega_2$  beams, and  $A_1$  and  $A_2$  are the corresponding input beam cross-sections.  $A_3$  is the cross-section of the  $\omega_3$  beam.  $T_1$ ,  $T_2$ , and  $T_3$  are the single surface transmission coefficients at  $\omega_1$ ,  $\omega_2$ , and  $\omega_3$  respectively.  $L$  is the length of the crystal.  $\alpha_1$ ,  $\alpha_2$ , and  $\alpha_3$  are the power absorption coefficients at  $\omega_1$ ,  $\omega_2$ , and  $\omega_3$  respectively.

Using CO<sub>2</sub> laser lines  $\omega_1 = 1045.02 \text{ cm}^{-1}$  (P22) and  $\omega_2 = 945.98 \text{ cm}^{-1}$  (P18) with  $P_{\omega_1} \approx P_{\omega_2} \approx 3 \text{ MW}$  and  $A_1 \approx A_2 \approx A_3 \approx 1 \text{ cm}^2$ , the output energy

was measured to be 1 mJ per pulse at  $\omega_3 = 1144.06 \text{ cm}^{-1}$ . This corresponds<sup>10</sup> to  $P_{\omega_3} = 10 \text{ kW}$ . Using a value<sup>2</sup> of  $1.5 \times 10^{-10} \text{ esu} \pm 50\%$  for  $\chi_{1111}^{(3)}$ ,  $n_1 \approx n_2 \approx n_3 = 4$ ,  $L = 8.3 \text{ cm}$ ,  $\alpha_1 \approx \alpha_2 \approx \alpha_3 \approx 0.03 \text{ cm}^{-1}$ , Eq. (5) predicts a value of 22 kW for  $P_{\omega_3}$ . This is in agreement with the measured value of 10 kW considering the large uncertainty in the value of  $\chi_{1111}^{(3)}$  and similar uncertainties in our peak power measurements.

For a practical application of this technique for the uranium isotope separation, there are two important considerations:

(a) Does this technique provide the proper IR wavelength in the  $8.62 \mu\text{m}$  region for the separation in  $\text{UF}_6$ ? A partial list of wavelengths in the  $8.62 \mu\text{m}$  region along with the two input  $\text{CO}_2$  laser frequencies  $\omega_1$  and  $\omega_2$  is given in Table I. As can be seen from Table I, there are a number of IR frequencies around  $8.62 \mu\text{m}$ . Even if none of these satisfies the wavelength requirement, many more frequencies can be obtained by using three input  $\text{CO}_2$  laser frequencies  $\omega_1$ ,  $\omega'_1$ , and  $\omega_2$  such that the IR frequency would be given by  $\omega_3 = \omega_1 + \omega'_1 - \omega_2$ .

(b) Will this technique meet the energy requirements? Assuming that the  $8.62 \mu\text{m}$  excitation is at least as efficient as the  $12.1 \mu\text{m}$  excitation, the energy requirements<sup>7</sup> are in the range of 10 - 100 mJ per pulse. In the present experiment, we obtained an output of 1 mJ per pulse using external  $\text{CO}_2$  laser power inputs  $P_{\omega_1} = P_{\omega_2} = 3 \text{ MW}$  in a  $1 \text{ cm}^2$  cross-section. According to Eq. (5),  $P_{\omega_3}$  is proportional to  $(P_{\omega_1})^2 P_{\omega_2}$ . Since the damage threshold of intrinsic germanium is of the order of  $100 \text{ MW/cm}^2$ , one can safely increase the input power density to  $10 \text{ MW/cm}^2$  for each of the  $\text{CO}_2$  laser beams. The output energy should then increase to 37 mJ per pulse. The output energy

can be further increased by a factor of  $\sim 5$  to 185 mJ per pulse by AR coating the input and output faces of the germanium crystal. This would correspond to a 4.6 % efficiency for conversion of the  $\text{CO}_2$  laser radiation into the  $8.6 \mu\text{m}$  radiation. If one considers 10 % efficiency for the  $\text{CO}_2$  lasers, the net conversion efficiency will be 0.46 % which is above the 0.1 % level anticipated for economic feasibility.<sup>7</sup> Further increases in the efficiency should be possible by increasing the length of the crystal beyond 8.3 cm used in the present experiment. Since large germanium crystals are available, the total energy at a given conversion efficiency could be scaled up by using germanium crystals with larger cross-section along with correspondingly bigger  $\text{CO}_2$  lasers.

Similar 4-photon mixing experiments were also attempted for the generation of radiation at  $\omega_3 = 2\omega_2 - \omega_1$  in the  $12 \mu\text{m}$  region. Again using  $P_{\omega_1} \simeq P_{\omega_2} \simeq 3 \text{ MW}$  with  $A_1 \simeq A_2 \simeq A_3 = 1 \text{ cm}^2$ ,  $\omega_1 = 1045.02 \text{ cm}^{-1}$ , and  $\omega_2 = 945.98 \text{ cm}^{-1}$ ,  $P_{\omega_3}$  at  $\omega_3 = 846.94 \text{ cm}^{-1}$  ( $11.81 \mu\text{m}$ ) was determined to be  $\sim 150 \text{ W}$  in contrast to a calculated value of 12 kW. We are currently looking into this large discrepancy between calculated and observed values.

Finally we would like to point out that several thousand different combinations of frequencies can be obtained with 4-photon noncollinear mixing in germanium by choosing different lines for the two input  $\text{CO}_2$  lasers. Orders of magnitude more combinations of frequencies can be obtained by using three different  $\text{CO}_2$  lasers. Thus this 4-photon mixing may prove to be a very versatile and practical technique for the generation of step-tunable coherent radiation in the 8 to  $13 \mu\text{m}$  region.

References:

1. C.K.N. Patel, R.E. Slusher, and P.A. Fleury, Phys. Rev. Letters 17, 1011 (1966).
2. J.J. Wynne and G.D. Boyd, Appl. Phys. Letters 12, 191 (1968).
3. S.S. Jha and N. Bloombergen, IEEE J. Quant. Electronics QE-4, 670 (1968).
4. J.J. Wynne, Phys. Rev. 178, 1295 (1969).
5. R.N. Hall, in Proceedings of the Twelfth International Conference on the Physics of Semiconductors, Stuttgart, 1974 (B.G. Teubner, Stuttgart, 1974), p. 363.
6. E.D. Capron and O.L. Brill, Appl. Optics 12, 569 (1973).
7. R.J. Jensen, J.G. Marinuzzi, C.P. Robinson and S.D. Rockwood, Laser Focus, May 1976, p. 51.
8. C.D. Salzberg and J.J. Villa, J. Opt. Soc. Am. 47, 244 (1957).
9. N. Lee, R.L. Aggarwal, and B. Lax, Appl. Phys. Letters 29, 45 (1976).
10. The input peak powers given here have been deduced on the assumption that half of the CO<sub>2</sub> pulse energy is contained in an initial spike of 100 nsec (FWHM) with the remaining half of the energy in a relatively long tail. The output peak powers were obtained by assuming that the output energy was contained in a 100 nsec (FWHM) pulse.

TABLE I. Partial List of IR frequencies  $\omega_3 = 2\omega_1 - \omega_2$  between 8.614  
and 8.626  $\mu\text{m}$  obtained from 4-photon mixing of  $\text{CO}_2$  laser  
lines  $\omega_1$  and  $\omega_2$

$\lambda_3$ ( $\mu\text{m}$ )	$\omega_3$ ( $\text{cm}^{-1}$ )	$\omega_1$ ( $\text{cm}^{-1}$ )	$\omega_2$ ( $\text{cm}^{-1}$ )
8.6146	1160.814	1069.014 (R 6)	977.214 (R22)
8.6151	1160.748	1046.854 (P20)	932.960 (P32)
8.6168	1160.518	1048.661 (P18)	936.804 (P28)
8.6169	1160.515	1071.884 (R10)	983.252 (R32)
8.6182	1160.335	1050.441 (P16)	940.548 (P24)
8.6192	1160.197	1052.196 (P14)	944.194 (P20)
8.6199	1160.105	1053.924 (P12)	947.742 (P16)
8.6203	1160.058	1055.625 (P10)	951.192 (P12)
8.6203	1160.055	1057.300 (P 8)	954.545 (P 8)
8.6206	1160.011	1070.462 (R 8)	980.913 (R28)
8.6208	1159.989	1073.278 (R12)	986.568 (R38)
8.6240	1159.556	1069.014 (R 6)	978.472 (R24)
8.6253	1159.384	1071.884 (R10)	984.383 (R34)
8.6258	1159.316	1043.163 (P24)	927.008 (P38)

Figure Captions

Fig. 1. Wave vector diagram for the noncollinear 4-photon mixing of laser beams of frequencies  $\omega_1$  and  $\omega_2$  to generate phase-matched radiation at  $\omega_3 = 2\omega_1 - \omega_2$ .  $\vec{k}_1$ ,  $\vec{k}_2$ , and  $\vec{k}_3$  are the wave vectors of the  $\omega_1$ ,  $\omega_2$ , and  $\omega_3$  beams respectively.

Fig. 2. Schematic of the experimental setup for the noncollinear 4-photon mixing of CO<sub>2</sub> laser beams of frequencies  $\omega_1$  and  $\omega_2$  to generate infrared radiation at  $\omega_3 = 2\omega_1 - \omega_2$  in germanium. For  $\omega_1 = 1045 \text{ cm}^{-1}$  and  $\omega_2 = 946 \text{ cm}^{-1}$ , the external phase-matching angles were found to be  $\theta_E \simeq 2.2^\circ$  and  $\varphi_E = 1.8^\circ$ .

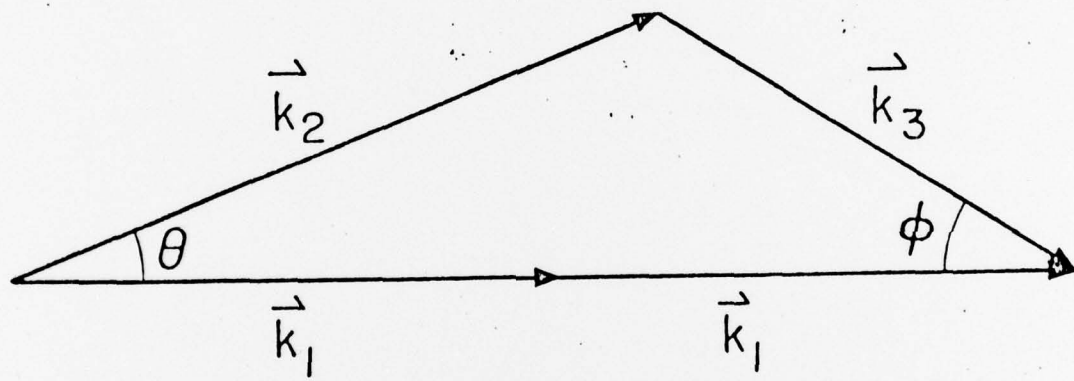


Fig. 1  
Lee, Aggarwal, and Dex

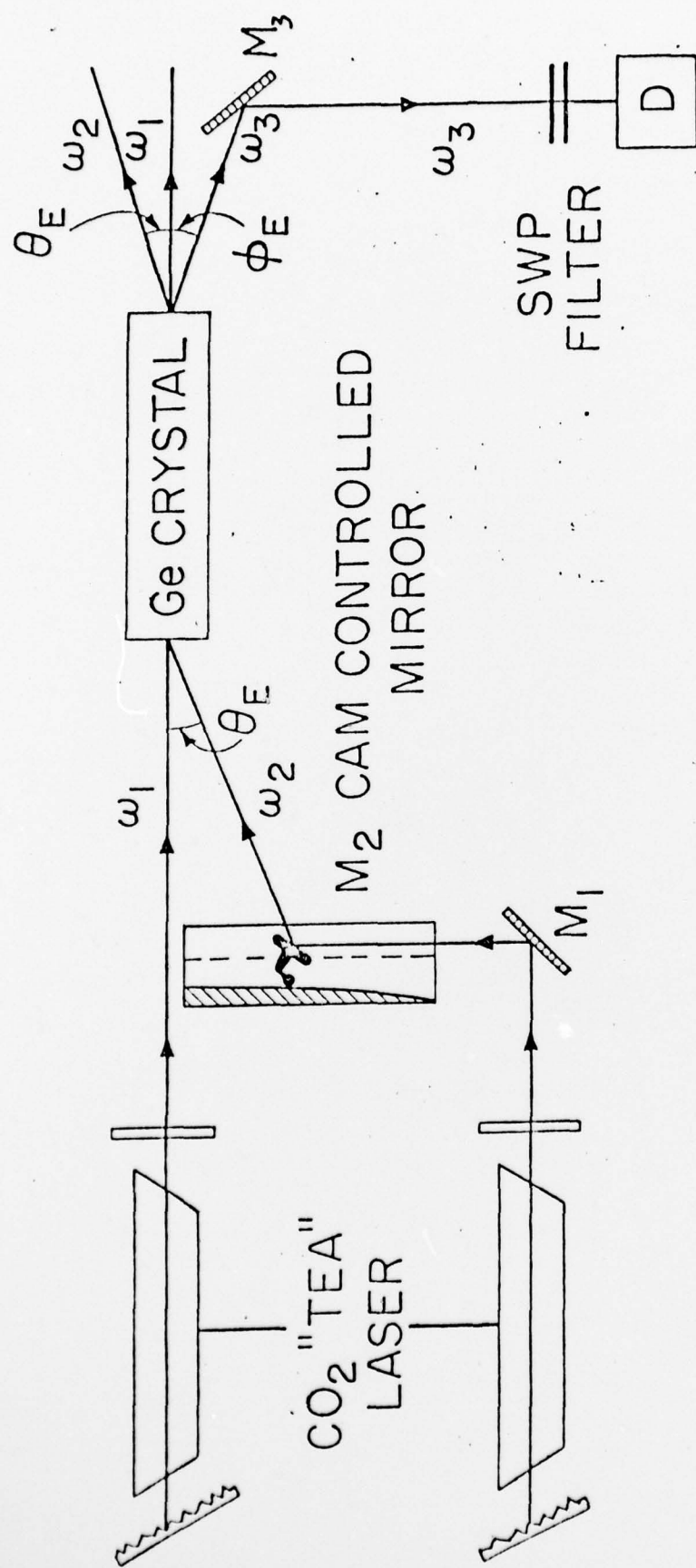


Fig. 2  
 Lee, Agnew, and Lee

APPENDIX D

Efficient High-Power 8.62  $\mu\text{m}$  Infrared Radiation Source  
for Uranium Isotope Separation in  $\text{UF}_6$

(To appear in Proceedings of the International Conference  
on Lasers and Their Applications, Leon, Norway, 1976)

Efficient High-Power 8.62  $\mu\text{m}$  Infrared Radiation Source for  
Uranium Isotope Separation in  $\text{UF}_6$  \*

R. L. AGGARWAL†, N. LEE, and B. LAX†

Francis Bitter National Magnet Laboratory‡  
Massachusetts Institute of Technology  
Cambridge, Massachusetts 02139

Introduction

This paper examines various aspects of the generation of infrared radiation at 8.62  $\mu\text{m}$  by noncollinear phase-matched four photon mixing of  $\text{CO}_2$  laser beams in germanium at room temperature, as a potential infrared source for the uranium laser isotope separation in  $\text{UF}_6$ .

The success of the two-step laser isotope separation in  $\text{UF}_6$  will depend, ultimately, on the development of efficient, high-power narrow-band tunable infrared (IR) radiation sources. In this laser isotope separation scheme, the  $\text{U}^{235}\text{F}_6$  molecule is first selectively excited to a higher vibrational energy level by the absorption of an IR photon followed by the absorption of a higher-energy photon in the ultraviolet (UV) region. The important selective IR absorption bands in  $\text{UF}_6$  occur at 15.9  $\mu\text{m}$ , 12.1  $\mu\text{m}$ , 8.62  $\mu\text{m}$ , and 7.74  $\mu\text{m}$ , which correspond, respectively to the  $\nu_3$ ,  $\nu_3 + \nu_5$ ,  $\nu_3 + \nu_2$ , and  $\nu_3 + \nu_1$  vibrational transitions [1, 2]. Here  $\nu_3$  is an IR-active mode and  $\nu_1$ ,  $\nu_2$  and  $\nu_5$  are the Raman-active modes of  $\text{UF}_6$  [3]. According to JENSEN et al. [1], the pulse energy requirements for the IR laser source range from several millijoules at 15.9  $\mu\text{m}$  to tens of millijoules at 8.62  $\mu\text{m}$  with a linewidth of less than 0.05  $\text{cm}^{-1}$ . For economic feasibility of the enrichment program, the efficiency of the IR source should be in excess of 0.1% at a pulse repetition exceeding 500 pps.

So far, emphasis has been placed on the generation of the 15.9  $\mu\text{m}$  radiation since the cross-section for absorption at the 15.9  $\mu\text{m}$  fundamental band is about a hundred times larger than that at the 12.1  $\mu\text{m}$ , 8.62  $\mu\text{m}$ , and 7.74  $\mu\text{m}$  combination bands. Unfortunately, various methods employed to-date have provided 15.9  $\mu\text{m}$  radiation pulses with energy in the 100- $\mu\text{J}$  level which is about an order of magnitude below the energy requirement of several mJ [1]. On the other hand, the present 4-photon mixing scheme appears to satisfy not only the pulse energy requirements but also the efficiency, repetition rate, frequency and linewidth requirements.

\*Supported in part by the Massachusetts Institute of Technology Funds and in part by the Advanced Research Projects Agency through the Office of Naval Research

†Also Department of Physics, Massachusetts Institute of Technology

‡Supported by the National Science Foundation

### Noncollinear 4-Photon Mixing

Recently we have reported [4] the achievement of phase-matching in 4-photon mixing of  $\text{CO}_2$  laser beams in germanium using the noncollinear mixing geometry. The wave vector diagram for noncollinear phase-matching is shown in Fig. 1. Here  $\vec{k}_1$  and  $\vec{k}_2$  are the wave vectors for the input laser beams of frequencies  $\omega_1$  and  $\omega_2$  respectively;  $\vec{k}_3$  is wave vector for the radiation generated at the frequency  $\omega_3 = 2\omega_1 - \omega_2$  for  $\omega_1 > \omega_2$ . Using the refractive index data for germanium [5], the angles  $\theta$  and  $\phi$  are determined to be less than  $1^\circ$ . Using this method approximately 1 mJ of energy per pulse was obtained at  $8.7 \mu\text{m}$  from an 8.3 cm long crystal of germanium with  $1 \text{ cm}^2$  cross-section and  $3 \text{ MW/cm}^2$  peak input intensity from each of two  $\text{CO}_2$  TEA lasers operating at the frequencies  $\omega_1$  and  $\omega_2$ . The output energy can be scaled up through the use of higher input intensities and longer crystals of germanium.

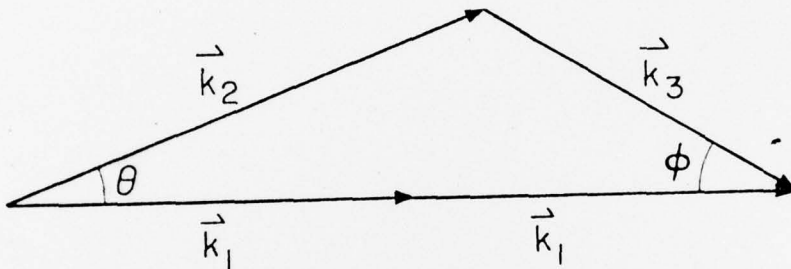


Fig. 1. Wave vector diagram for noncollinear phase-matched 4-photon mixing

Since the damage threshold of germanium is approximately  $100 \text{ MW/cm}^2$ , one can conservatively increase the input intensity to  $10 \text{ MW/cm}^2$  for each of the two input beams. The output energy which is proportional to the third-power of the input intensity will scale up to 37 mJ per pulse. Another factor of 5 increase in the output energy to 185 mJ can be readily obtained by anti-reflection coating of the input and output surfaces of the germanium crystal.

Under the phase-matched condition, the maximum effective length of the crystal is limited by the absorption of the crystal. The absorption coefficient  $\alpha$  of optical grade germanium, as shown in Fig. 2, is less than  $0.03 \text{ cm}^{-1}$  in the  $8 \mu\text{m}$  to  $11 \mu\text{m}$  region. So one should be able to obtain useful mixing lengths of about 30 cm. Therefore the output energy can be further increased to  $\sim 400 \text{ mJ}$  by increasing the length of the mixing crystal from 8.3 cm to 20 cm. This would correspond to  $\sim 1\%$  efficiency for conversion from the electrical power into the  $8.62 \mu\text{m}$  infrared radiation, assuming 5% efficiency for the  $\text{CO}_2$  lasers. Such a source is well above the minimum energy requirement of tens of mJ and minimum efficiency of 0.1% for the uranium enrichment program. Furthermore, it is obvious to see that the output power can be linearly scaled up with input beams of the same intensity but larger cross-section.

A typical atmospheric TEA laser has a gainwidth of 3 GHz or  $0.1 \text{ cm}^{-1}$  and its output consists of several longitudinal modes. Thus the resulting output of the 4-photon mixing with these typical  $\text{CO}_2$  TEA lasers may exceed the  $0.05 \text{ cm}^{-1}$  linewidth requirement for the selective isotope excitation of the  $\text{UF}_6$  molecule. However, single longitudinal mode operation in  $\text{CO}_2$  lasers can be obtained by using the hybrid laser scheme [6] in which the laser cavity contains both a low pressure discharge tube and a high pressure TEA section. Due to the narrow linewidth of the low pressure medium, the hybrid system is forced to oscillate in a single longitudinal

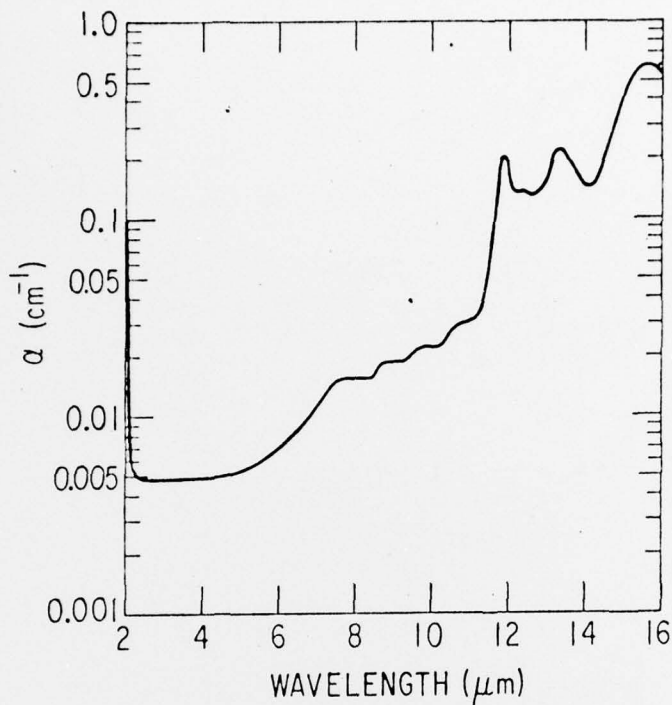


Fig. 2. Absorption coefficient  $\alpha$  of optical grade germanium at room temperature, as supplied by Eagle-Picher

mode. There is an alternative scheme to obtain single longitudinal mode action in a  $\text{CO}_2$  TEA laser. Recently, we have demonstrated [7] single longitudinal mode operation with fine tuning capability over the pressure broadened gainwidth of the  $\text{CO}_2$  laser by using a tilted intracavity GaAs etalon. The advantage of this scheme is that it does not only provide single longitudinal mode to satisfy the linewidth requirement but can also provide fine frequency tuning as large as  $0.3 \text{ cm}^{-1}$  which would be useful to optimize the frequency of the  $8.62 \mu\text{m}$  radiation for the uranium separation. However, the losses due to the insertion of an intracavity etalon and laser operation at a frequency away from the center of the gain curve would reduce the efficiency of the  $\text{CO}_2$  laser system.

In Fig. 3, we show a number of lines which can be obtained in the  $8.62 \mu\text{m}$  region by mixing two  $\text{CO}_2$  laser lines. If one uses three input  $\text{CO}_2$  lasers for mixing instead, on the order of a thousand different combinations can be obtained in that same small frequency range of Fig. 3. Therefore it should be possible to select the desired wavelength in the  $8.62 \mu\text{m}$  region by using two or three  $\text{CO}_2$  lasers.

For the high repetition rate of 500 pulses per second, one has to consider heat dissipation capability of the crystal. For a projected total of 2 to 3 joules per pulse  $\text{CO}_2$  laser input energy, and a maximum absorption coefficient of  $0.03 \text{ cm}^{-1}$ , the power absorbed by a  $20 \text{ cm}$  long crystal would be 600 W at the repetition rate of 500 pps. If the crystal is held between two copper blocks maintained at room temperature, the rise in temperature,  $\Delta T$ , at the center of the crystal with respect to the temperature of the copper blocks is given by

$$\Delta T = \frac{tQ}{8KA} \quad (1)$$

where  $t$  is the thickness of the germanium crystal,  $Q$  is the power dissipated by the two surfaces,  $K$  is the thermal conductivity of the germanium crystal at room temperature and  $A$  is the area of contact between the crystal and the cold finger. Using the values  $t = 1$  cm,  $Q = 600$  W and  $K = 0.5$  W cm $^{-1}$  K $^{-1}$ , (1) predicts  $\Delta T = 6.4^\circ\text{K}$ , assuming perfect thermal contact between germanium and copper. Thus it appears that germanium should be able to handle high repetition rates of several hundred pulses per second.

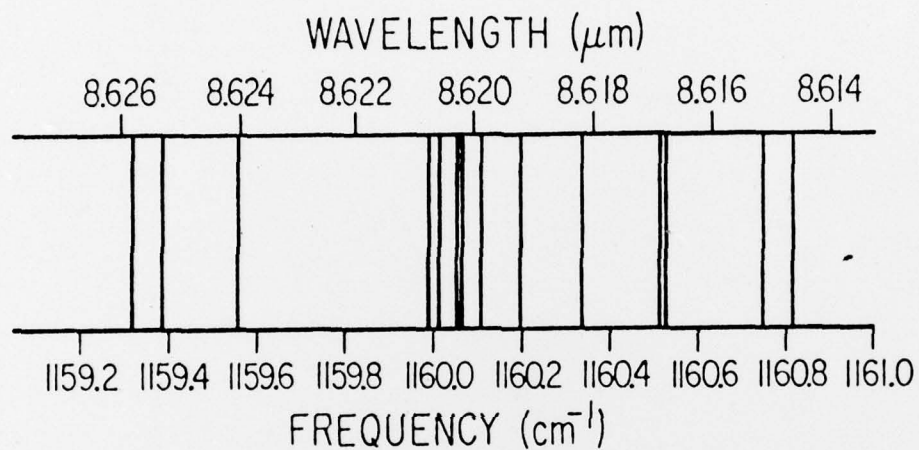


Fig. 3. Infrared lines obtainable in the 8.62  $\mu\text{m}$  region by 4-photon mixing of two  $\text{CO}_2$  laser lines

In summary, the noncollinear 4-photon mixing of  $\text{CO}_2$  lasers in germanium can provide an infrared source consistent with the requirements for the uranium isotope separation program in  $\text{UF}_6$ .

#### Acknowledgments

We wish to thank Mr. J. Reising of Eagle-Picher for supplying the absorption spectrum of germanium.

#### References:

1. R.J. Jensen, J.G. Marinuzzi, C.P. Robinson and S.D. Rockwood, *Laser Focus*, May 1976, p. 51.
2. J.W. Eerkens, *Appl. Phys.* 10, 15 (1976).
3. For the normal modes of an octahedral  $\text{XY}_6$  molecule, see for example, G. Herzberg, *Molecular Spectra and Molecular Structure*, Vol. II (Van Nostrand Reinhold Company, New York, 1945), p. 51.
4. N. Lee, R.L. Aggarwal and B. Lax (Submitted to *Appl. Phys. Lett.*)
5. C.D. Salzberg and J.J. Villa, *J. Opt. Soc. Am.* 47, 244 (1957).
6. A. Gondhalekar, E. Holzhauer, and N.R. Heckenberg, *Phys. Lett.* 46A, 229 (1973).
7. N. Lee, R.L. Aggarwal, and B. Lax (unpublished).